1999-01-3653

Particulate Matter Measurements in a Diesel Engine Exhaust by Laser-Induced Incandescence and the Standard Gravimetric Procedure

David R. Snelling, Gregory J. Smallwood, Robert A. Sawchuk, W. Stuart Neill, Daniel Gareau, Wallace L. Chippior, Fengshan Liu, and Ömer L. Gülder
National Research Council Canada
ICPET Combustion Research Group

William D. Bachalo
Artium Technologies

ABSTRACT

Laser-induced incandescence has emerged as a promising technique for measuring spatially and temporally resolved particulate volume fraction and size. Laser-induced incandescence has orders of magnitude more sensitivity than the gravimetric technique, and thus offers the promise of real-time measurements and adds the increasingly desirable size and morphology information. Particulate matter emissions have been measured by laser-induced incandescence and the standard gravimetric procedure in a mini dilution tunnel connected to the exhaust of a single-cylinder diesel engine. The engine used in this study incorporates features of contemporary medium- to heavy-duty diesel engines and is tuned to meet the U.S. EPA 1994 emission standards. The engine experiments have been run using the AVL 8-mode steady-state simulation of the U.S. EPA heavy-duty transient test procedure. Results of the measurements using the two methods are compared and the suitability of the laser-induced incandescence for particulate mass measurements in diesel exhaust is demonstrated.

INTRODUCTION

A significant portion of atmospheric particulates arises from combustion of fuels in various engines and furnaces. In urban areas, mobile sources are major contributors to ambient particulate matter (PM) concentrations. The main constituent of the particulates generated by combustion is carbon. These carbonaceous particulates, which are produced from gas-phase combustion processes, are generally called soot, and those that form as a result of direct pyrolysis of liquid hydrocarbon fuels are generally referred to as coke or cenospheres.

The detrimental effect of soot particulates on human health is a current concern and various restrictions are being placed on particulate matter emissions from vehicles and other sources. From an operational point of view, soot formation is not desired in most power plants.

The particulate emissions from diesel engines are in the form of complex aerosols consisting primarily of soot and volatile organics. There is limited information currently available on the size and morphology of diesel particulates; most measurements have been for concentration only. However, soot itself has been studied in more detail. Most soot particles are agglomerates of 5 to 30 nm diameter primary particles. Typical dimensions of these agglomerates range from 10 to 1000 nm, but most of the mass is log-normally distributed with mass median diameters on the order of 100 to 250 nm [1,2]. These dimensions of the diesel soot particles are very similar to those obtained from atmospheric diffusion flames of gaseous hydrocarbon fuels [3-5]. As the particulate concentrations in the exhaust of modern diesel engines are reduced, the agglomerate sizes are also being decreased.

Figure 1 shows the average composition of the typical diesel exhaust particulate matter. Inorganic components in the diesel exhaust are products of engine and component wear, or are trace contaminants of the fuel and the lubricant. The metals found in the particulate matter are primarily trace fuel contaminants such as antimony, arsenic, barium, beryllium, cobalt, and strontium. These substances will vaporize in the combustion chamber and then stick to particles in the exhaust stream [6].

For regulatory purposes, particulate matter emissions are defined as the mass of the matter that can be collected from a diluted exhaust stream on a filter kept at

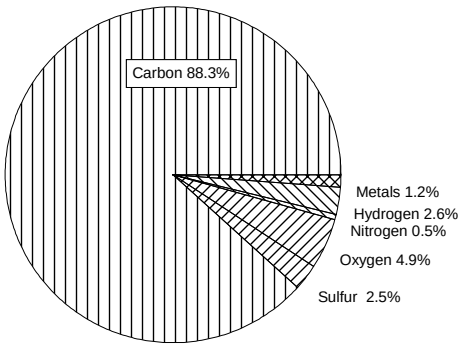

Figure 1. Elemental composition of the typical diesel particulate matter by mass.

52°C. This includes the organic compounds that condense at lower temperatures, but excludes the condensed water. Exhaust gas temperature, before the exhaust is diluted, plays an important role on the amount of adsorbed soluble organics; low exhaust gas temperatures produce PM with more soluble organics than PM measured from a high temperature exhaust [7].

This measurement gives the averaged PM emissions over the time period during which the particulates are collected on the filter. In spite of its drawbacks and limitations, the filter technique is being used for diesel engine and diesel fuel certification and testing. Since the collected PM and other condensed material on the filter aggregate, it is impractical to determine the particulate size and size distribution.

Laser-induced incandescence (LII) has emerged as a promising technique for measuring spatially and temporally resolved particulate volume fraction and size [8-18]. In LII, the particulates are heated by a short duration laser pulse. With sufficiently high laser energies, numerical models of the heat and mass transfer indicate that the particulates reach peak temperatures of 4000-4500 K [8,9,13,15,16]. The resultant incandescence, while of short duration, can be readily detected and processed to yield concentration and size information. LII typically has a temporal resolution of 10 ns and can be used to perform both quantitative point measurements and 2-D planar visualization. LII has orders of magnitude more sensitivity than the gravimetric technique, and thus offers the promise of real-time measurements and adds the increasingly desirable size and morphology information.

Particulate matter emissions have been measured by LII and the standard gravimetric procedure in a mini dilution tunnel connected to the exhaust of a single-cylinder DI research diesel engine. The engine used in this study incorporates features of contemporary medium- to heavy-duty diesel engines and is tuned to meet the U.S. EPA 1994 emission standards. The engine experiments have been run using the AVL 8-mode steady-state simulation of the U.S. EPA heavy-duty transient test procedure. Results of the measurements using the two methods are compared and the suitability of LII for particulate mass measurements is discussed.

BACKGROUND

SOOT PARTICULATE FORMATION IN COMBUSTION

The formation of soot particulate, i.e. the conversion of a hydrocarbon fuel with molecules containing a few carbon atoms into a carbonaceous agglomerate containing some millions of carbon atoms in a few milliseconds, is an extremely complex process. This process involves a transition from gaseous to solid phase where the solid phase does not exhibit any unique chemical and physical structure. The accepted mechanism for this process is as follows (see, e.g. [19-22]):

The hydrocarbon fuel goes through pyrolysis or partial oxidation during combustion and forms small hydrocarbon radicals from which small hydrocarbons, particularly acetylene(s), are formed. Reaction of C_4 species (e.g. diacetylene) with C_2 species (acetylene) produce a C_6 species which can form an aromatic structure through isomerization. It is also possible to have C_3H_3 dimerization with subsequent isomerization to an aromatic structure. The formation of larger aromatic rings occurs mainly via an acetylene addition mechanism. Coagulation of these larger aromatic ring compounds is proposed to account for the formation of primary soot particles. The smallest of these particles,

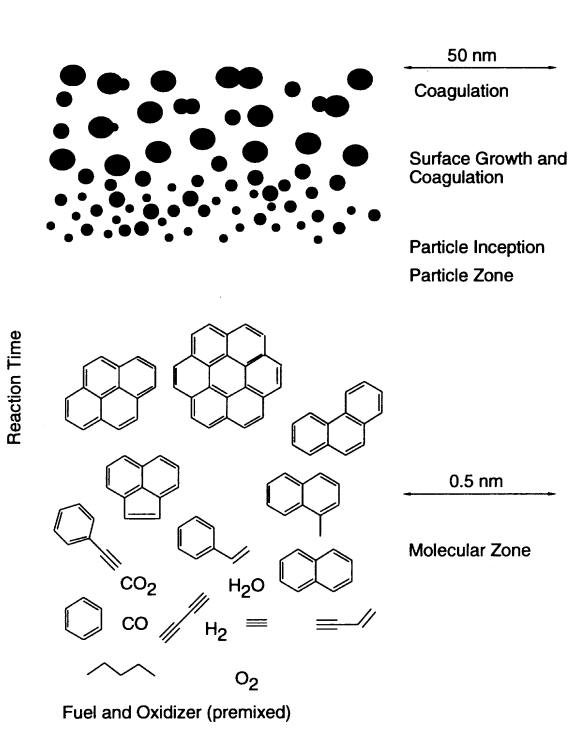

Figure 2. A schematic representation of soot formation in combustion [19].

when observed under the electron microscope, are about 1.5 nm in diameter, corresponding to a molecular mass of about 2000. These primary particles then pick up molecules from the gas phase promoting surface growth, whose rate is one of the determining factors in final soot concentration. The final size of the soot particles results from coagulation of primary particles to larger aggregates. A schematic representation is given in Figure 2.

EXHAUST PARTICULATE MEASUREMENTS

For regulatory purposes, the particulate matter in the exhaust is measured by collecting the PM on a filter in a dilution tunnel. This measurement gives the averaged PM emissions over the time period during which the particulates are collected on the filter. For exhausts containing lower concentrations of PM, the collection time could be very long for collecting enough PM for reasonable measurements. In spite of its drawbacks and limitations, the filter technique is being used for diesel engine and fuel certification and testing. Since the collected PM and other condensed material on the filter stick together, it is almost impractical to determine the particulate size and size distribution. However, the soluble organic fraction can be extracted from the collected material and analyzed for its chemical composition.

One of the principal instruments for particulate size measurements for particulates within an aerodynamic diameter range of 0.01 to 1 μm has been the differential mobility particle sizer (DMPS). This device separates charged particles according to their aerodynamic size using an electric field. Separated particles are then counted using a condensation nucleus counter which yields a number-weighted size distribution. Since the response time of the instrument is on the order of a minute, it is not suitable for transient measurements [23].

A fairly new instrument capable of measuring particle sizes in the 0.04 to 10 μm range is the electrical low-pressure impactor (ELPI). Particulates are first charged and then passed through a cascade impactor, which segregates them into a number of bins (size ranges). Changes in the current deposited on each impactor stage yield the transient concentrations of particles of the corresponding aerodynamic size [23].

NON-INTRUSIVE SOOT/PARTICULATE MEASUREMENTS

In combustion research soot volume fraction measurements are important for studies of soot formation, radiation processes, and for monitoring post-flame particulates. Light extinction is a commonly used diagnostic technique for measuring soot volume fraction. However, it suffers from the drawback of measuring a line-of-sight average, and while tomographic reconstruction can be used to calculate soot profiles in radially symmetric flames, this is not possible under turbulent flow conditions. Elastic scattering of light has been widely investigated for soot measurements but the fact that the signal is proportional to the sixth power of the particle diameter means that the technique is more useful for particle sizing than volume fraction measurements. More importantly, for agglomerated soot particles (which are definitely not spherical), it has become increasingly clear in the last few years that the approach of applying Mie theory by assuming spherical soot particles results in large errors [24-27].

By combining the elastic scattering and extinction techniques it is possible to obtain the soot particulate morphological parameters. Köylü [28] describes an *in situ* particulate diagnostic technique based on the Rayleigh-Debye-Gans polydisperse fractal aggregate scattering interpretation of absolute angular light scattering and extinction measurements. Using the proper particle refractive index, the method yields particle volume fraction, fractal dimension, primary particle diameter, particle number density, and aggregate size distribution [28]. However, the technique is complex (the absolute scattering cross-section must be measured as a function of scattering angle) and is limited to laminar cases (laminar flames and laminar gas flows) and cannot be used in turbulent environments.

LII uses a pulsed focused laser beam to provide an instantaneous (about 10 ns) energy source. Several mJ of energy is used to rapidly heat particulates to their evaporation temperature. The soot particulates radiate incandescence as they cool back to the ambient temperature, which is about 1500 to 2000 K in flames, and is much less in a diesel exhaust. The incandescence signal is collected and imaged onto a detector as a function of time. This signal is proportional

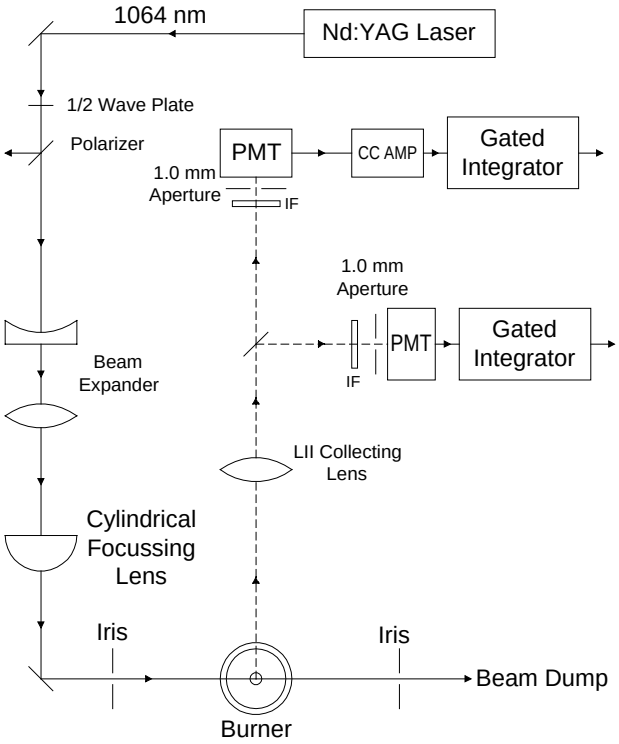

Figure 3. Schematic of the LII setup at NRC [18].

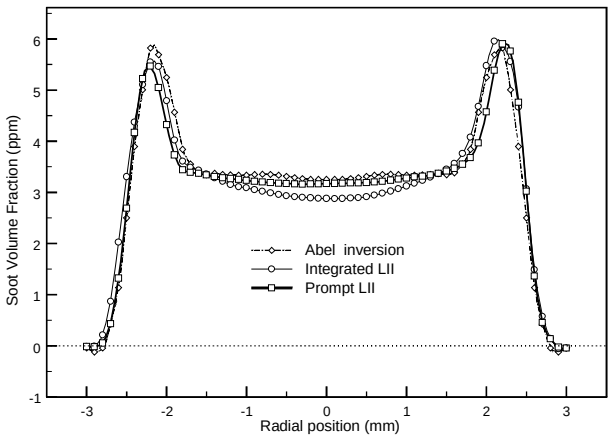

Figure 4. Comparison of soot volume fraction determined by LII to radial profiles from Abel inversion of line-of-sight extinction data at 40 mm above the burner in a laminar diffusion flame of ethylene and air [18].

to the particulate volume fraction over a very wide dynamic range and it is also possible to determine the particulate size [18]. It can be used in any environment, including laminar and turbulent flames and exhaust gas streams. The schematic of the LII setup at NRC is shown in Figure 3. Figure 4 shows a comparison of measurements of soot volume fraction in a laminar diffusion flame by LII and by line-of-sight extinction. A brief description of the LII theory is given in the Appendix.

EXPERIMENTAL

TEST ENGINE AND EXHAUST EMISSION MEASUREMENTS

The engine used in this work is a single-cylinder research version (Ricardo Proteus) of a Volvo TD123 heavy-duty truck engine. The engine is a direct-injection type and had a displacement volume of 2 liters. Major engine configuration data are shown in Table 1. The research engine incorporates many features of contemporary medium- to heavy-duty diesel engines. It is tuned to meet the U.S. EPA 1994 emission standards.

The speed and the load of the research engine were controlled independently by a dynamometer and a fuel control system. To simulate a turbo charger, externally compressed and dried air, controllable for temperature and pressure, was supplied to the engine. The exhaust system was fitted with an orifice downstream of the exhaust port, which, together with the exhaust back pressure valve, provided a cylinder pressure pumping loop similar to that of the multi-cylinder parent engine. A mixing tank in the exhaust line reduced the pressure/flow pulsations and provided complete mixing of the exhaust gases before sampling.

Table 1. Research Engine Configuration

Engine Type	Ricardo Proteus (replicates one cylinder of Volvo D123)
Bore	130.2 mm
Stroke	150.0 mm
Number of Cylinders	1
Displacement	1.997 litres
Combustion Chamber Type	Toroidal Bowl
Compression Ratio	17:1
Number of Valves/Cylinder	2
Injection Type	Direct Injection
Fuel Injection Pump	Bosch PE6P 120A 320RS8011
Injection Pressure (Typical)	120 MPa (17,400 psi)
Fuel Injection Nozzle	Bosch DLLA 152 P 285
Maximum Power Output	44.67 kW (60 bhp) @ 1900 rev/min

Filtered lubricating oil was delivered to the engine by external pump. The temperature of the engine oil was controlled to 80°C. The engine coolant temperature was controlled at 80°C.

A Kistler 6121 high-temperature pressure transducer was mounted in the research engine to measure cylinder pressure. The fuel injector was instrumented with a Wolff hall-effect needle-lift sensor so that the start and the end of fuel injection could be determined. The engine crankshaft position was determined by an AVL 360C/720S high-resolution optical crank angle encoder.

A heated probe was mounted after the exhaust surge tank to sample the gaseous emissions. The emissions instrumentation (Rosemount, model NGA 2000) consisted of a chemiluminescent oxides of nitrogen (NO_x) analyzer, a flame ionization total hydrocarbon (HC) analyzer, a non-dispersive infrared carbon monoxide (CO) analyzer, a paramagnetic oxygen (O_2) analyzer, and a non-dispersive infrared carbon dioxide (CO_2) analyzer for measuring the CO_2 concentration in the dilution tunnel. A non-dispersive infrared CO_2 analyzer (Horiba, model MEXA-211GE) was used to measure the CO_2 concentration in the engine exhaust.

A separate probe was used to sample the particulate emissions. The temperature of the particulate probe was maintained at 190^{o}C to prevent condensation of the heavy hydrocarbons. The exhaust sample was diluted in a mini-dilution tunnel using filtered and dried air. The flow rate of the dilution air was regulated to maintain a temperature of 52^{o}C. A particulate sampling line was installed in the dilution tunnel and connected to a 47 mm particulate filter and a volume meter. A computer running a data acquisition software recorded engine control parameters and emission values. A total of 60 data points were recorded in duration of 5 minutes. Averaged

Table 2. AVL 8-Mode Steady-State Simulation of EPA Transient Test Procedure

Mode	Speed (rpm)	Load (%)	Weighting Factor
1	600	0	35.01
2	743	25	6.34
3	873	63	2.91
4	1016	84	3.34
5	1900	18	8.40
6	1835	40	10.45
7	1835	69	10.21
8	1757	95	7.34

values of speed, power, fuel consumption rate, temperatures, pressures and exhaust emission concentrations were used in the calculation of composite emissions.

To establish a link of the results from this work to those obtained with the EPA transient test procedure, the AVL 8-mode steady-state simulation test procedure was adopted [29]. The engine operating conditions and the weighting factors of this test procedure are listed in Table 2. The engine speed in this test procedure varies widely, from low idle speed (600 rpm) to rated speed (1900 rpm). The load also varies widely from 0% to 95%. The low idle condition is weighted heavily in the test procedure. In calculating the composite brake specific emissions, the weighting factor (WF) at each mode is used in the following equation:

$$BSE = \frac{\sum (Emission\ Rate)_i \times WF_i}{\sum (Brake\ Power)_i \times WF_i} \qquad (1)$$

The emission rates in the equation are calculated from measured emission concentrations and fuel consumption rates.

To make the engine experimental results relevant to multi-cylinder production engines, an effort was made to run the research engine at operating conditions as closely as possible to the "parent" production engine. The research engine manufacturer supplied the speed and load mapping of the multi-cylinder "parent" engine. Using this information, engine speed, torque, intake manifold temperature, intake manifold pressure, intake airflow, engine brake torque and exhaust back pressure were determined. Further details of the engine and the conventional particulate measurements are given in [30-32].

LII MEASUREMENT SYSTEM

The LII system that was described previously [18], Figure 3, has been modified for diesel exhaust particulate matter measurements. Briefly, a pulsed Nd:YAG laser, operating with 16 mJ/pulse at 20 Hz and 1064 nm, was used to heat the particulates to their evaporation temperature. A half-wave plate to rotate the plane of polarization in combination with a thin film

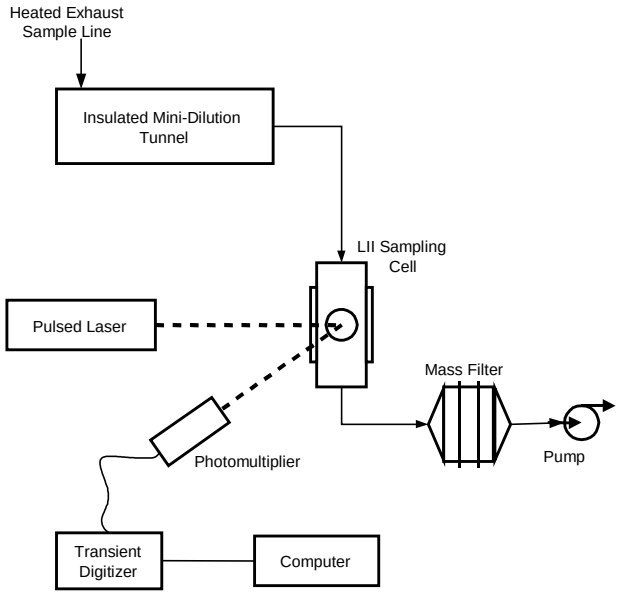

Figure 5. General layout of the LII exhaust particulate matter measurement system.

polarizer angle-tuned to transmit horizontally polarized radiation was used to control the laser energy.

The beam was then focused with a cylindrical lens to form a sheet through the probe volume. The beam intensity profiles in the probe volume were measured with a Coherent BeamView system. These profiles were used to ensure that the laser fluence was just beyond the saturation threshold for raising most of the soot particles to the evaporation temperature.

The LII signal from the centre of the laser sheet was imaged at 0.5:1 magnification with an achromatic 31.5 mm diameter lens of 80 mm focal length onto an optical fibre of 600 μm diameter, which transmitted the incandescence signal to the photomultipliers. The imaging system was arranged such that the imaging axis was at an angle of 35° to the plane of the laser sheet. Thus the sample volume in the flame was a slanted cylinder of diameter 1.2 mm whose mean length was 2.1 mm.

The LII signal was recorded by three photomultipliers, equipped with narrowband interference filters centered at 402 nm (36 nm FWHM), 551 nm (18 nm FWHM), and 781 nm (19 nm FWHM), respectively. Prompt signals from the photomultipliers, 10 ns duration and at the LII signal peak, were recorded and subsequently transferred to a computer for further analysis. Multipulse averages were acquired, with 400, 500, or 1000 samples per average, depending upon the particulate load. Between 3 and 5 averages were collected during each trial, and three trials were performed for each of the eight engine modes.

A sampling cell for producing and acquiring the LII signal was inserted between the dilution tunnel and the filters used for gravimetric sampling. This cell (Fig. 5) provided one window for introducing the laser beam and signal

collection, a second window for passing the laser beam to a beam dump, and a third window orthogonal to the laser beam for viewing and alignment. The laser sheet was centered 2 mm from the end of the tube carrying the exhaust from the dilution tunnel. The LII data was recorded simultaneously with the gravimetric sampling, to provide a direct relationship between the two measurements of PM.

RESULTS AND DISCUSSION

Repeatability of the LII measurements of the particulate matter in the exhaust of the single-cylinder diesel engine is shown in Figure 6. Each bar represents the mean of 3 to 5 multiple averages acquired during a single trial. At engine modes 1,2,6, and 8, all three LII measurements collapse into single points. The largest spread is at engine mode 4. At all modes, however, LII repeatability has been far superior to filter mass measurements.

Figure 7 shows the plot of LII measurements of particulate versus filter mass measurements. The good correlation between the two measurements demonstrates the capabilities of the LII system. The scatter observed in Fig.7 could be caused by several factors. One of the most significant ones is the amount of the soluble organic fraction of the diesel particulate matter at a given engine mode. It should be noted that LII produces signals at much lower particulate concentrations than other techniques, an advantage with modern cleaner diesel engines.

The soluble organic fraction in the diesel particulate matter could vary from 5 to 40% by mass depending on the sampling train and the engine operating conditions, among other variables. The residence time of the particulate matter, through the sampling system just before it is captured on filter, as well as the temperature of the exhaust gas before it is diluted plays an important role in the amount of unburned hydrocarbons in the exhaust stream adsorbed into the particulate matter. The standard gravimetric filter measurements include the mass of the adsorbed organics in the mass of the particulate matter. However, in LII measurements, the organics adsorbed into the particulate matter evaporate very rapidly as the laser pulse starts heating the particulates within the probe volume. Thus the LII signal contains only the information proportional to the mass of the carbon in the particulate matter (neglecting any effect of the trace metals in the particulates may have).

These results confirm the suitability of the LII technique for standardized particulate matter measurements in diesel engine exhausts. Recent work by other groups has demonstrated, although without comparison to standard techniques, the suitability of LII for soot mass concentration measurements in the exhaust of a diesel powered vehicle [33] and in an environment similar to that of a gas turbine exhaust [34].

CONCLUDING REMARKS

Particulate matter emissions have been measured by LII and the standard gravimetric procedure in a mini dilution tunnel connected to the exhaust of a single-cylinder DI research diesel engine. The engine experiments have been run using the AVL 8-mode steady-state simulation of the U.S. EPA heavy-duty transient test procedure. A semi-portable LII system developed and designed at the National Research Council of Canada has been used for the LII measurements. Results of the measurements using the two methods are compared and it was shown that:

1. The repeatability of the LII measurements is far better than the repeatability of the standard gravimetric filter technique.
2. The LII measurements show good correlation with

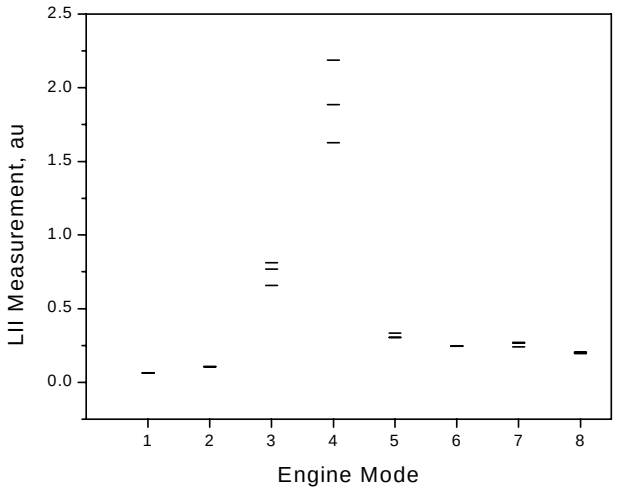

Figure 6. Repeatability of LII measurements of exhaust particulate matter at different engine modes.

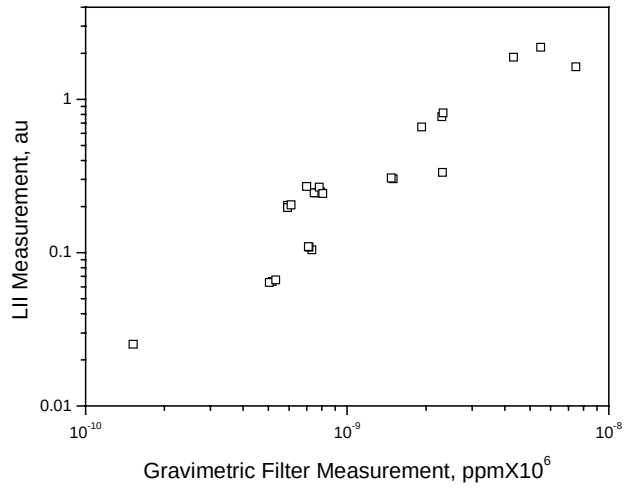

Figure 7. Correlation between the LII measurements and the standard gravimetric filter measurements of the exhaust particulate matter. Data cover the measurements made at all of the 8 engine modes.

the filter mass measurements over a wide range of operating conditions and particulate levels.

In addition, LII is capable of real-time particulate matter measurements which covers any engine transient operation. The wide dynamic range and lower detection limit of LII make it a potential standard instrument for particulate matter measurements. LII has also the potential to give information about the size and morphology of the particulate matter. Use of LII also provides a significant time advantage both in the collection and processing of data, over the gravimetric procedure.

ACKNOWLEDGMENTS

Partial funding for this work has been provided by the Canadian Governments PERD Program's Particulates Initiative (Advanced Transportation Task), Syncrude Canada Ltd., Shell Canada Ltd., and Imperial Oil Ltd.

CONTACT

The authors Snelling (dave.snelling@nrc.ca), Smallwood (greg.smallwood@nrc.ca), Sawchuk, Neill, Gareau, Chippior, Liu, and Gülder (omer.gulder@nrc.ca) are with the National Research Council Canada, ICPET Combustion Research Group, Building M-9, 1200 Montreal Road, Ottawa, Ontario K1A 0R6, Canada (www.icpet.nrc.ca/combustion), and the author Bachalo (wbachalo@aol.com) is with Artium Technologies, 14660 Saltamontes Way, Los Altos Hills, California 94022, USA (www.artium.com).

REFERENCES

1. Dolan, D. F., Kittelson, D. B., and Pui, D. Y. H. "Diesel Exhaust Particle Size Distribution Measurement Techniques", SAE Paper No. 800187, 1980.
2. Williams, R. L., 1982, "Diesel Particulate Emissions", in Toxicological Effects of Emissions from Diesel Engines, (J. Lewtas (Ed.)), Elsevier, New York, pp.15-32, 1982.
3. Megaridis, C. M., and Dobbins, R. A., "Soot Aerosol Dynamics in A Laminar Ethylene Diffusion Flame", 22nd Symposium (International) on Combustion, The Combustion Institute, pp.353-362, 1988.
4. Dobbins, R. A., and Subramaniasivam, H., "Soot Precursor Particles in Flames" in Soot Formation in Combustion (Bockhorn, H., (Ed.)), Springer-Verlag, Berlin, pp.290-299, 1994.
5. Megaridis, C. M., and Dobbins, R. A. "Comparison of Soot Growth and Oxidation in Smoking and Non-Smoking Ethylene Diffusion Flames", Combust. Sci. Technol. 66, pp.1-16, 1989.
6. Anon., "Unregulated Motor Vehicle Exhaust Gas Components", Volkswagen AG, Research and Development (Physico-Chemical Metrology). Project coordinator: K. H. Lies. 3180 Wolfsburg 1, Germany, 1989.
7. Kishi, Y., Tohno, H., and Ara, M.,"Characteristics and Combustibility of Particulate Matter", in Reducing Emissions from Diesel Combustion, Society of Automotive Engineers, Warrendale, PA. pp. 139-146, 1992.
8. Dasch, C. J., "New Soot Diagnostics in Flames Based on Laser Vaporization of Soot", 20th Symposium (International) on Combustion, The Combustion Institute, pp.1231-1237, 1984.
9. Melton, L. A., "Soot Diagnostics Based on Laser Heating", Appl. Optics, 23, pp.2201-2208, 1984.
10. Dec, J. E., zur Loye, A. O., and Siebers, D. L., "Soot Distribution in a D.I. Diesel Engine Using 2-D Laser Induced Incandescence Imaging", SAE Transactions, 100, pp.277-288, 1991.
11. Vander Wal, R. L., and Weiland, K. J., "Laser-Induced Incandescence: Development and Characterization Towards a Measurement of Soot Volume Fraction", Appl. Phys. B59, pp.445-452, 1994.
12. Puri, R., Richardson, T. F., Santoro, R. J., and Dobbins, R. A., "Aerosol Dynamic Processes of Soot Aggregates in a Laminar Ethene Diffusion Flame", Combust. Flame, 92, pp.320-333, 1993.
13. Hofeldt, D. L., "Real-Time Soot Concentration Measurement Technique for Engine Exhaust Streams", SAE Paper No. 930079, 1993.
14. Bengtsson, P. E., and Alden, M., "Soot Visualization Strategies Using Laser Techniques: Laser-Induced Fluorescence in C2 from Laser-Vaporized Soot and Laser-Induced Soot Incandescence", Appl. Phys. B 60, pp.51-59, 1995.
15. Mewes, B. S., and Seitzman, J. M., "Soot Volume Fraction and Particle Size Measurements with Laser-Induced Incandescence", Appl. Optics, 36, pp.709-717, 1997.
16. Tait, N. P., and Greenhalgh, D. A., "PLIF Imaging of Fuel Fraction in Practical Devices and LII Imaging of Soot", Berichte der Bunsengesellschaft für Physikalische Chemie, 97, pp.1619-1625, 1993.
17. Will, S., Schraml, S., and Leipertz, A., "Two-Dimensional Soot Particle Sizing by Time-Resolved Laser-Induced Incandescence", Optics Lett. 20, pp.2342-2344, 1995.
18. Snelling,D. R., Smallwood, G. J., Campbell, I. G., Medlock, J. E., and Gülder, Ö. L., "Development and Application of Laser Induced Incandescence (LII) as a Diagnostic for Soot Particulate Measurements", Proceedings of the NATO/AGARD Propulsion and Energetics Panel, 90th Symposium on Advanced Non-Intrusive Instrumentation for Propulsion Engines, 20-24 October, 1997, Brussels, Belgium.
19. Bockhorn, H. (Ed.), Soot Formation in Combustion, Springer-Verlag, Berlin, 1994.
20. Glassman, I., "Soot Formation in Combustion Processes", 22nd Symposium (International) on Combustion, The Combustion Institute, p.295-310, 1988.
21. Glassman, I., 1996, Combustion, 3rd Edition, Academic Press, San Diego, Chap.8, 1996.
22. Frenklach, M., and Wang, H., "Detailed Mechanism and Modelling of Soot Particle Formation" in Soot Formation in Combustion (Bockhorn, H., (Ed.), Springer-Verlag, Berlin, pp.165-192, 1994.

23. Anon., "Formation and Characterization of Particles: Report of the 1996 HEI Workshop", Health Effects Institute HEI Communications, Number 5, September 1997.

24. Dobbins, R. A., and Megaridis, C. M., "Morphology of Flame-Generated Soot as Determined by Thermophoretic Sampling", Langmuir, 3, pp.254-259, 1987.

25. Dobbins, R. A., and Megaridis, C. M., "Absorption and Scattering of Light by Polydisperse Aggregates", Appl. Optics, 30,pp.4747-4754, 1991.

26. Köylü, Ü. Ö., and Faeth, G. M., "Optical Properties of Overfire Soot in Buoyant Turbulent Diffusion Flames at Long Residence Times", J. Heat Trans., 116, pp.152-159, 1994.

27. Köylü, Ü. Ö., and Faeth, G. M., "Optical Properties of Soot in Buoyant Laminar Diffusion Flames," J. Heat Trans. 116, pp.971-979, 1994.

28. Köylü, Ü. Ö., "Quantitative Analysis of In Situ Optical Diagnostics for Inferring Particle / Aggregate Parameters in Flames: Implications for Soot Surface Growth and Total Emissivity", Combust. Flame, 109, pp.488-500, 1996.

29. Cartellieri, W. P. and Herzog, P. L., "Swirl Supported or Quiescent Combustion for 1990's Heavy-Duty DI Diesel Engines - An Analysis", SAE Paper 880342, 1988.

30. Li, X., Chippior, W. L. and Gülder, Ö. L., "Effects of Fuel Properties on Exhaust Emissions of a Single Cylinder DI Diesel Engine", SAE Paper 962116, 1996.

31. Li, X., Chippior, W. L. and Gülder, Ö. L., "Effects of Cetane Enhancing Additives and Ignition Quality on Diesel Engine Emissions", SAE Paper 972968, 1997.

32. Li, X., Chippior, W. L., Gülder, Ö. L., Cooley, J., Richardson, E. K., and Mitchell, K., "Comparison of the Exhaust Emissions of Diesel Fuels Derived from Oil Sands and Conventional Crude Oil", SAE Paper No. 982487, 1998.

33. Schraml, S., Will, S., and Leipertz, A., "Simultaneous Measurement of Soot Mass Concentration and Primary Particle Size in the Exhaust of a DI Diesel Engine by Time-Resolved Laser-Induced Incandescence (TIRE-LII)", SAE Paper 1999-01-0146, 1999.

34. Wainner, R. T., Seitzman, J. M., and Martin, S. R., "Soot Measurements in a Simulated Engine Exhaust Using Laser-Induced Incandescence", AIAA Journal, 37, pp 738-743,1999.

APPENDIX

LII THEORY - HEAT TRANSFER TO AND FROM SOOT PARTICLES

The numerical modeling of the transient heating and subsequent radiation and cooling of soot particles exposed to short duration (10 ns) laser pulses is briefly described below. The approach is similar to that used by several authors [9, 13, 15, 16]. Our approach most closely follows that of Hofeldt [13] and only the differences between the two models will be emphasized.

The previous LII numerical modeling has assumed the particles to be equivalent spheres and calculated the absorption from Mie theory [8, 9, 13, 16]. In recent years it has become clear that Mie theory based on equivalent spheres introduces large errors in calculating the scattering and absorption of real soot particles [24, 25, 26, 27] (and references contained therein), and that soot absorption is well described by Rayleigh theory, provided that the primary particle diameter is within the Rayleigh limit (significantly smaller than the light wavelength).

The equations describing the soot heat transfer presented here are for a more realistic soot morphology in that we assume the soot particles to be agglomerates of N_P just touching primary particles of diameter d_P [24]. This approach has also been recently adopted by Mewes et al [15].

The heat transfer energy balance equation is:

$$C_a q - \frac{2 K_a (T - T_0) \pi N_P d_P^2}{(D_{ES} + G \lambda_{MFP})} + \frac{H_v}{M_V} \frac{dM}{dt} + q_{rad} - \frac{1}{6} \pi N_P d_P^3 \rho_S c_s \frac{dT}{dt} = 0 \quad \text{(A1)}$$

The first term, $C_a q$, is the absorbed laser energy, where, in the Rayleigh limit, the absorption cross section C_a is given by:

$$C_a = \frac{\pi^2 N_P d_P^3 E(m)}{\lambda} \quad \text{(A2)}$$

This will certainly be true in our experiments since we are clearly in the Rayleigh limit, having used 1064 nm laser excitation.

The second term involves heat transfer to the surrounding medium for a particle in the transition regime between continuum and free molecule (Knudsen) heat transfer. Since the mean free path in the gas is typically much larger than the soot particle diameter, the particle is largely in the free molecule limit, and thus the heat transfer coefficient is independent of particle size. G is a geometry dependent heat transfer factor, equal to $8f/(\alpha(\gamma+1))$ where f is the Eucken factor (5/2 for monatomic species), α is the accommodation coefficient, and $\gamma=c_p/c_v$ (= 1.40 for air). A value of α~0.9 has generally been adopted in previous work [9, 13, 16].

The third term is heat loss due to evaporation of the soot and is given by:

$$\frac{dM}{dt} = \frac{\rho_s}{2} \pi D^2 \frac{dD}{dt} = -\pi N_P d_P^2 \frac{\frac{P_S(T) N_{AV}}{RT}}{\frac{1}{\beta}\left(\frac{2\pi M_V(T)}{RT_S}\right)^{1/2} + \frac{D_{ES}}{2 D_{AB}}} \quad \text{(A3)}$$

Again the flux of carbon vapour is dominated by the free molecule regime (the first term in the denominator of Eq. A4) and is independent of particle size. The soot vapour pressure has generally been calculated using fixed

values of the heat of vaporisation H_v and soot vapour molecular weight M_V. We have used the temperature dependent values of these quantities $P_S(T)$, $M_V(T)$ calculated using empirical relationships in solving the equations.

The fourth term, representing radiative loss for a single primary particle, can be approximated as:

$$q_{rad_p} = 4\pi^2 N_P d_P^3 \sigma_{SB} T^4 \left(\frac{E(m)}{\lambda} \right)_{600} \qquad \text{(A4)}$$

where the expression in parentheses is evaluated at some average wavelength, 600 nm in this case. This approximation, including the selection of evaluation wavelength, is not limiting since soot particle heat loss due to radiation is insignificant compared to the other heat loss terms.

The particle equivalent sphere diameter dependence (D_{ES}) in the denominator of Eqs. A2 and A4 is the equivalent sphere diameter given by $D^3_{ES}=N_p \cdot d^3_p$ and it reflects the dependence of heat transfer and the flux of evaporating soot on this soot size in the continuum limit. Since the soot particle diameter is very much less than the gas mean free path these continuum terms are not important and for soot evaporation have been neglected in much of the earlier modelling [9, 16]. In our approach, these equations constitute a coupled set of differential equations for D and T that have been solved numerically using a Runge-Kutta integration routine. From this solution we can calculate the time history of the LII signal using the relationship:

$$I(\lambda) = \frac{2\pi c^2 h}{\lambda^5} \left[e^{\frac{hc}{k\lambda T}} - 1 \right]^{-1} \pi N_P d_P^2 K_{ap}(\lambda) d\lambda$$
$$\text{where } K_{ap} = \frac{4\pi d_P E(m)}{\lambda} \qquad \text{(A5)}$$

The LII signal I is a function of T, d_P, N_P, time (t), and laser fluence (F). To calculate values of I to compare with experiment we must integrate I over the range of laser fluence values encountered in the laser sheet. Since our probe volume only occupies a small region of the sheet the distribution of laser fluence is essentially constant in the plane of the sheet. However, there is a distribution of fluence across the thickness of the sheet (i.e. along the LII viewing axis). This can be described by

$$F(x) = F_0 \exp\left(-\frac{x^2}{w_x^2} \right) \qquad \text{(A6)}$$

where w_x is the sheet half width and F_0 is the peak fluence at the centre of the sheet. $I(F,t)$ can then be integrated across these fluence values to give a signal $I_G(t)$ that can be compared to our experiments. The prompt and integrated LII signal for a given laser fluence can be obtained by the appropriate time integration of $I_G(t)$.